

Numerical evidence for Kosterlitz–Thouless transition in the 2D XY Villain model

W. Janke and K. Nather

Institut für Theoretische Physik, Freie Universität Berlin, Arnimallee 14, W-1000 Berlin 33, Germany

Received 22 April 1991; accepted for publication 8 May 1991

Communicated by A.A. Maradudin

Using the single cluster Monte Carlo algorithm combined with improved estimators for correlation functions we have simulated the two-dimensional XY model in Villain's formulation on large square lattices with up to 1200×1200 sites. Weighted least-squares fits of the correlation length ($10 < \xi < 140$) and susceptibility near criticality clearly favor the exponential divergence predicted by Kosterlitz and Thouless. A conventional power-like critical behavior can be ruled out on a statistically firm basis.

Two-dimensional (2D) systems with short-range interactions and continuous symmetry are disordered for all non-zero temperatures [1]. Still, for $O(2)$ symmetric systems, the Kosterlitz–Thouless (KT) theory [2] (for reviews see ref. [3]) predicts a peculiar “topological” phase transition governed by an essential singularity. Accordingly, as the critically temperature T_c is approached from high temperatures, the correlation length ξ and susceptibility χ diverge *exponentially*,

$$\xi \propto \exp(bt^{-\nu}), \quad \chi \propto \xi^{2-n}, \quad (1)$$

while the specific heat should stay finite at T_c . Here $t \equiv T/T_c - 1 > 0$ is the reduced temperature, $b \approx 1.5$ is a non-universal constant, and $\nu = \frac{1}{2}$, $\eta = \frac{1}{4}$ are universal critical exponents. In the physical picture underlying the KT theory, the transition is caused by the dissociation of vortex–antivortex pairs at T_c . Below the critical temperature these pairs are tightly bound and merely renormalize the spin-wave excitations, which destroy long-range order down to zero temperature. Both the physical picture and the prediction (1) have been questioned many times [4,5]. Alternative considerations [5] favor *power-law* singularities of the form

$$\xi \propto t^{-\nu}, \quad \chi \propto t^{-\gamma}, \quad (2)$$

with conventional critical exponents ν and γ

($= \nu(2-\eta)$). The goal of this note is to decide between these two alternatives.

Recent studies in this direction employing high-temperature series expansions [6] and Monte Carlo (MC) simulations^{#1} are based on lattice models of the planar XY type with local spin–spin interactions taken in the so-called cosine form,

$$\begin{aligned} E &= - \sum_{\mathbf{x}, \mathbf{i}} s(\mathbf{x}) \cdot s(\mathbf{x} + \mathbf{i}) \\ &= - \sum_{\mathbf{x}, \mathbf{i}} \cos[\nabla_{\mathbf{i}} \theta(\mathbf{x})], \end{aligned} \quad (3)$$

where $s = (\cos \theta, \sin \theta)$, and $\nabla_{\mathbf{i}} \theta(\mathbf{x}) \equiv \theta(\mathbf{x} + \mathbf{i}) - \theta(\mathbf{x})$ are the lattice gradients in the \mathbf{i} direction of a simple square lattice. It is well known that, with this energy, vortex and spin-wave degrees of freedom are coupled in a complicated non-linear way [11]. Both approaches favor the KT scenario, but the MC results could not give the last degree of certainty.

The KT arguments and subsequent analyses [12,13] on the other hand assume (sometimes implicitly) that vortices and spin waves are decoupled. While universal properties should be insensitive to this assumption, it is quite conceivable that the quantitative approach of criticality does depend on

^{#1} Gupta et al. [7], using an over-relaxation algorithm; Wolff [8], using the single cluster update, but conventional observables; Edwards et al. [9], using multigrid MC. For earlier work, using the Metropolis algorithm, see ref. [10].

the vortex spin-wave coupling. We found it therefore worthwhile to investigate the issue of an exponential versus power-law critical behavior once more by MC simulations of a related model in which vortices and spin waves are explicitly decoupled, namely the periodic Gaussian or Villain model [14]. Its partition function reads

$$Z = \prod_x \left(\int_{-\pi}^{\pi} \frac{d\theta(x)}{2\pi} \right) \times \sum_{\{n_i(x)\}} \exp\left(-\frac{\beta}{2} \sum_{x,i} (\nabla_i \theta - 2\pi n_i)^2\right), \quad (4)$$

where the integer variables $n_i(x)$ run from $-\infty$ to ∞ , and $\beta \equiv 1/T$ is the inverse temperature. From a recent study [15] (for earlier work, see also ref. [16]) of the dual discrete Gaussian model the location of the critical point is known to be around $\beta_c \approx 0.74$. A thorough MC study appeared feasible, since the application of recently developed cluster algorithms [17,18] combined with low-variance estimators for correlation functions [19] promised a speed-up by several orders of magnitude as compared to the standard Metropolis algorithm. Indeed, in this note we shall present data for the correlation length and susceptibility of the Villain model (4) that are (i) considerably more accurate than previous results for the cosine model (3), and (ii) invade much deeper into the critical region.

In our MC simulations we worked with the single-cluster (1C) algorithm of ref. [18] slightly adapted to the Villain case. While the necessary modifications are easy to write down analytically, their actual evaluation is much more time-consuming than for the cosine model. In order to reduce computer-time requirements we have therefore employed the Z_N (with $N=100$) approximation of the $O(2)$ symmetry, which is known to be extremely accurate and which is straightforward to implement in the cluster algorithm.

In this brief note we shall concentrate on our measurements of the zero-momentum ("projected") correlation function,

$$g(|x-x'|) \equiv \frac{1}{L} \sum_{y,y'=1}^L \langle s(x,y) \cdot s(x',y') \rangle, \quad (5)$$

and the susceptibility,

$$\chi \equiv V \left\langle \left(\frac{1}{V} \sum_x s(x) \right)^2 \right\rangle \quad (6)$$

in the high-temperature phase. Here $V=L \times L$ is the volume of our square lattices (with periodic boundary conditions), and the angular brackets denote averages with respect to the partition function (4). As sample estimators for g and χ we have used the "cluster observables" [19]

$$\hat{g} = \frac{1}{L} \sum_{y,y'=1}^L 2 \frac{V}{C} \mathbf{r} \cdot \mathbf{s}(x) \mathbf{r} \cdot \mathbf{s}(x') \Theta_c(x) \Theta_c(x'), \quad (7)$$

$$\hat{\chi} = \frac{1}{L} \sum_{x,x'=1}^L \hat{g} = 2C \left(\frac{1}{C} \sum_{x \in \mathcal{C}} \mathbf{r} \cdot \mathbf{s}(x) \right)^2, \quad (8)$$

where \mathbf{r} is the random unit vector used in the (stochastic) construction of the cluster \mathcal{C} of reflected spins ($s \rightarrow s' = s - 2\mathbf{r}(\mathbf{r} \cdot \mathbf{s})$), C is the size or weight of the cluster, and $\Theta_c(x)$ denotes its characteristic function ($=1$ if $x \in \mathcal{C}$ and 0 otherwise). The factor 2 accounts for the $O(2)$ symmetry. It has been demonstrated [19] that $\langle \hat{g} \rangle = g$, $\langle \hat{\chi} \rangle = \chi$, and argued (or verified numerically for the $O(3)$ model [19]) that averages over many cluster steps have much smaller variances than the conventional estimators in (5), (6).

These arguments remain valid for the Z_N approximation if one keeps the trivial single-site clusters (generated for $\mathbf{r} \perp \mathbf{s}(x_0)$). Alternatively, since trivial single-site clusters only replicate the old configurations in a uniform way, one may avoid them by a suitable prescription in the update procedure. Then the factor 2 has to be replaced by $2 - 2/N$. This gives a smooth interpolation between the Ising ($Z_2 = O(1)$) and XY ($Z_\infty = O(2)$) model. A useful check of these relations is provided by the identity $1 = 2 \langle C^{-1} \sum_{x \in \mathcal{C}} [\mathbf{r} \cdot \mathbf{s}(x)]^2 \rangle$.

From $g(x)$ we have extracted the correlation length ξ by weighted least-squares fits to a hyperbolic cosine,

$$g(x) = a \cosh[(L/2 - x)/\xi] \quad (x \gg 1), \quad (9)$$

thereby taking properly into account the periodic boundary condition. To avoid systematic errors due to "higher mass" states with smaller correlation lengths, we have discarded all $g(x)$ with $x < \xi$ in these fits. We have checked that discarding all points with $x < 2\xi$ yields statistically consistent results. Since this naturally increases the error bars (by a factor of

≈ 1.3), we have always quoted the former fits. The error bars were estimated by the usual binning procedure, i.e., by decomposing the whole run into large non-overlapping blocks of many measurements of $g(x)$, determining ξ for each block, and calculating the variance.

The main results of our simulations are given in table 1, where we have compiled the raw data for the correlation length and susceptibility in the high-temperature phase. Only data points with $\xi > 10$ are taken into account. To avoid finite-size effects, we have carefully chosen our lattice sizes to satisfy the condition $L > 8\xi$ (except for one instance with $L = 7.3\xi$). Quite elaborate finite-size scaling analyses for $\beta = 0.55$ ($\xi \approx 6$) and $\beta = 0.63$ with L/ξ varying from ≈ 4 to ≈ 14 clearly confirm that this is a very safe condition ($L > 6\xi$ would probably suffice also). It is one of the main advantages of the single cluster algorithm combined with the "cluster estimators" (7), (8) that an overly large lattice does not increase the run-time (apart from a small equilibration overhead). On the average, in each update step only $\langle C \rangle$ spins are reflected and simultaneously used for the measurements, independent of L . The true limiting factor is now the memory requirement. In table 1 we give the ratio $\langle C \rangle / \chi$, which is roughly constant as for the co-

sine model [8] and approaches ≈ 0.8105 for $\xi > 40$. Also given is the total run-time in units comparable to Metropolis sweeps ($t_{\text{run}} = \text{number of cluster steps} \times \langle C \rangle / V$). We have adjusted the run-time to ensure that all errors are less than 0.25%. From a "simulation of our simulation" we knew that under this condition it is very improbable to misinterpret a true exponential behavior as a power law by chance. Note that the reverse question is not meaningful, since the power law (2) is a special limiting case of the exponential ansatz (1).

In the final analysis we focused on the question whether our data in table 1 support a KT transition governed by an exponential divergence (1) or a conventional transition with a pure power-law singularity (2). In order to decide between the two alternatives, we have performed χ^2 -fits to ξ and χ . To be precise, we have fitted our 18 data points to the logarithms of the hypotheses (1) or (2),

$$\log \xi(T) = A + b(T/T_c - 1)^{-\nu} \quad (\text{KT}), \quad (10)$$

or

$$\log \xi(T) = A - \nu \log(T/T_c - 1) \quad (\text{power}), \quad (11)$$

with similar expressions for χ . Furthermore, we can rewrite these expressions also as functions of β . Near

Table 1

Correlation length ξ , susceptibility χ , and mean cluster size $\langle C \rangle$ in the high-temperature phase. $t_{\text{run}} = \text{number of cluster steps} \times \langle C \rangle / L^2$ is the total run-time in units comparable to Metropolis sweeps.

β	L	L/ξ	$t_{\text{run}}/10^3$	ξ	χ	$\langle C \rangle / \chi$
0.590	200	17.81	39.58	11.231(16)	177.74(17)	0.811544
0.595	200	16.24	69.63	12.313(11)	207.49(16)	0.811415
0.600	200	14.74	39.01	13.567(19)	244.36(27)	0.811261
0.605	200	13.34	73.61	14.991(14)	289.82(26)	0.811126
0.610	200	12.03	88.72	16.625(15)	345.94(31)	0.811045
0.615	200	10.76	76.68	18.591(20)	417.93(44)	0.810937
0.620	200	9.60	89.06	20.831(22)	509.21(56)	0.810858
0.625	400	16.98	19.51	23.563(37)	628.78(84)	0.810773
0.630	400	14.92	15.14	26.812(50)	784.2(1.4)	0.810678
0.635	400	12.99	21.27	30.786(52)	995.1(1.7)	0.810644
0.640	400	11.22	21.72	35.638(65)	1278.9(2.4)	0.810603
0.645	400	9.62	26.27	41.597(81)	1665.2(3.3)	0.810572
0.650	400	8.14	34.93	49.160(88)	2221.8(4.4)	0.810536
0.655	600	10.23	21.00	58.68(12)	3015.7(6.4)	0.810514
0.660	600	8.45	21.51	70.97(15)	4190(10)	0.810488
0.665	800	9.15	24.93	87.42(17)	6015(13)	0.810479
0.670	800	7.28	35.50	109.91(21)	8896(20)	0.810457
0.675	1200	8.57	19.37	139.97(30)	13604(33)	0.810457

Table 2

χ^2 fits of the data for the correlation length ξ and susceptibility χ to the KT and power-law hypotheses (10), (11). The argument of ξ and χ indicates the specific form of the ansatz, and Q is the standard goodness-of-fit parameter.

	Fit	χ^2	Q	A	b	β_c	ν
unconstrained KT fits (14 d.o.f.)	$\xi(T)$	9.41	0.80	-1.89(37)	2.18(31)	0.7539(49)	0.532(55)
	$\xi(\beta)$	9.68	0.79	-5.5(1.4)	4.6(1.3)	0.7466(53)	0.353(68)
	$\chi(T)$	10.05	0.76	-1.53(29)	3.19(24)	0.7566(28)	0.588(32)
	$\chi(\beta)$	9.81	0.78	-6.32(90)	6.00(81)	0.7497(31)	0.421(40)
constrained KT fits: $\nu = \frac{1}{2}$ (15 d.o.f.)	$\xi(T)$	9.79	0.83	-2.117(15)	2.370(11)	0.75106(36)	0.5
	$\xi(\beta)$	13.87	0.54	-3.551(24)	2.812(14)	0.75814(40)	0.5
	$\chi(T)$	18.82	0.22	-2.460(14)	3.964(10)	0.74890(20)	0.5
	$\chi(\beta)$	13.39	0.57	-4.855(22)	4.702(13)	0.75591(23)	0.5
power-law fits (15 d.o.f.)	$\xi(T)$	257.20	4×10^{-46}	-0.5749(54)	-	0.71069(20)	1.8818(50)
	$\xi(\beta)$	65.96	2×10^{-8}	-1.638(11)	-	0.71915(26)	2.3610(79)
	$\chi(T)$	942.74	2×10^{-191}	0.1174(50)	-	0.70889(11)	3.1533(46)
	$\chi(\beta)$	250.33	1×10^{-44}	-1.6638(94)	-	0.71723(14)	3.9543(73)

T_c , in leading order, this amounts to replacing $T/T_c - 1$ by $1 - \beta/\beta_c$ in (10) and (11).

The resulting fit parameters are given in table 2. A glance at the entry displaying χ^2 immediately shows our main result – on the basis of the data in table 1 the power-law hypothesis can be ruled out with high confidence. Even the “best” $\chi^2 \approx 66$ for the $\xi(\beta)$ power-law fit corresponds to an extremely small goodness-of-fit parameter $Q \approx 2 \times 10^{-8}$ (recall that this is the probability to find a set of simulation data

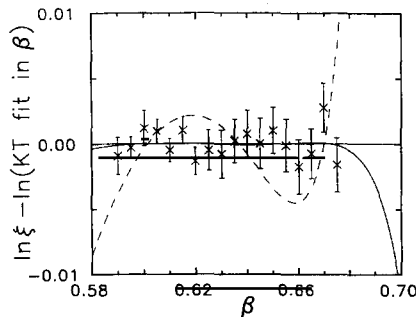


Fig. 1. KT fits (solid lines) and the β dependent power-law fit (dashed line) to the correlation length data, using the β dependent KT fit as a reference line. In a simple $\log \xi$ versus β plot, the three fits can hardly be distinguished. Note that in evaluating the fits it is not sufficient to simply insert the rounded values of the fitted parameters (with the significant digits determined by their individual error bars) as given in table 2. Due to the strong mutual correlations of the parameters (see fig. 2) it is necessary to use much higher precision values. The corresponding plot for the susceptibility looks very similar.

with $\chi^2 \geq 66$ by chance fluctuations, assuming that the power-law hypothesis is correct). On the other hand all KT fits look equally consistent with a χ^2 around 10. The quality of the fits can be inspected in fig. 1 (with the β -dependent KT fit as reference line). We interpret this result as unambiguous support for a KT-like transition in the 2D Villain model. Note that the currently available evidence against the power-law hypothesis from MC simulations of the cosine model is much weaker ($Q \approx 2 \times 10^{-3}$ for $\chi(\beta)$ [8]). Finally it should be stressed that statistical tests can in principle only provide evidence against a given hypothesis but never prove it in a strict sense. For example, a *generalized* power-law ansatz with additional confluent corrections yields good fits also, albeit with unreasonably large correction terms.

To be certain, we have performed all fits twice with (i) independently written programs using (ii) completely different algorithms, and (iii) running on two different computers (with 32 and 64 bit arithmetic). The power-law fits always agreed within a fraction of a percent. The KT fits require more care, but we never run into the “spurious minima” discussed in ref. [7]. In fact, since A and b enter as linear parameters in (10), we can easily determine their optimal values for fixed β_c and ν , and thus map out the χ^2 landscape over the $\beta_c - \nu$ plane. As a result, we find the approximately elliptic contour lines of constant χ^2 shown in fig. 2 which clearly imply a unique minimum. As a check, inserting the data of ref. [7] in

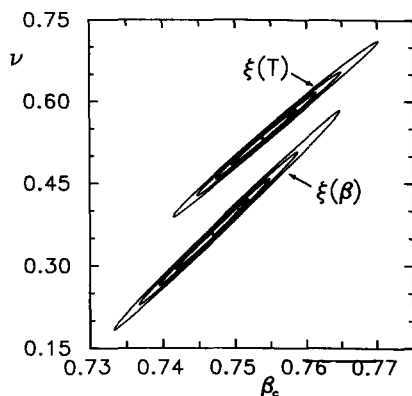


Fig. 2. Confidence regions in the β_c - ν plane for the KT fits to the correlation length data. Shown are the contour lines for $\Delta\chi^2 \equiv \chi^2 - \chi_{\min}^2 = 1, 2.30, 4.61, \text{ and } 9.21$. For a linear fit model and normally distributed errors, the projection of the $\Delta\chi^2 = 1$ region onto the axes gives the 68.3% confidence interval for a single parameter without regard to the other, while the other three regions are the 68.3%, 90%, and 99% confidence intervals for β_c and ν jointly [20]. For the non-linear KT fits this interpretation is only approximately valid.

our programs, we find KT fits which are again in agreement with each other but have smaller χ^2 than in ref. [7]. In particular, contrary to the claim in ref. [7], we have no problems with the β -dependent ansatz. On the other hand, we find much larger errors on the fit parameters. These errors are estimated [20] by drawing synthetic input data sets from Gaussian distributions with the measured variances, performing the fits and calculating the variance of the fitted parameters.

A closer look at the parameters reveals remaining problems with the KT fits. While the estimates for β_c are consistent with an overall mean

$$\beta_c = 0.752 \pm 0.005, \quad (12)$$

the estimates for ν show a systematic dependence on the form of the ansatz: the T -dependent fits give significantly larger values than the β -dependent fits, and the corresponding confidence regions in the β_c - ν plane shown in fig. 2 do not overlap. For the other two parameters, A and b , this discrepancy is even more pronounced. Unfortunately, since the χ^2 are almost equal for all KT fits, we have no numerical clue to decide which one is the best. Taking the average as best estimate, we get

$$\nu = 0.48 \pm 0.10, \quad (13)$$

where the (rough) error estimate accounts for the systematic shifts. This value is in fairly good agreement with the KT prediction. Using a constrained KT ansatz with fixed $\nu = \frac{1}{2}$ we also obtain fits with reasonable goodness-of-fit parameters (see table 2). When compared with the unconstrained ansatz, however, these fits do not look really acceptable. In addition we have tested the influence of the leading correction to the KT prediction for the susceptibility [13] #2, $\chi \propto \xi^{2-\eta} \rightarrow \chi \propto t^{-1/16} \xi^{2-\eta}$. As a result we get slightly modified parameters but do not find a further improvement of the fits.

The systematic errors of the parameters indicate that we are still too far away from the critical point, so that correction terms cannot be neglected. The numerical problem is that the KT fits do not signal this by a large χ^2 . Apparently they are able to absorb such corrections by generating effective parameters. We have verified this observation by a straightforward but tedious calculation which explains at least the sign and order of magnitude of the systematic shifts. Fig. 1 shows that even if the error bars are reduced by a factor of 10, we could not decide which KT fit is more trustworthy. Also, adding more measurements up to $\beta = 0.7$ with the present accuracy, say, would not help. But this already is extremely demanding, since the correlation length at $\beta = 0.7$ is roughly 770, thus requiring lattice sizes $L > 4500$ for a reliable simulation. These and similar estimates indicate that a significant improvement of the present results would require several months or even years of central-processing-unit (CPU) time on currently available computers such as the CRAY X-MP.

Let us finally use the second KT relation in eq. (1) to estimate the exponent η . A simple test of the theoretical prediction $\eta = \frac{1}{4}$ is a plot $\log(\chi/\xi^{7/4})$ versus $\log \xi$. A possible deviation $\Delta\eta \equiv \eta - \frac{1}{4}$ would be indicated by a straight line with slope $-\Delta\eta$. As is shown in fig. 3a this is obviously not the case. Rather, the data follow a curved line whose slope clearly decreases with increasing ξ , thus supporting the possibility that $\eta = \frac{1}{4}$ at the critical point. To demon-

#2 We thank Professor P. Butera for useful correspondence on this point.

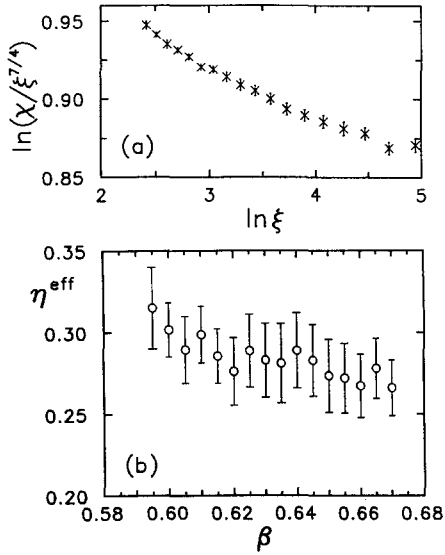


Fig. 3. Test of the KT prediction $\chi \propto \xi^{2-\eta}$ with $\eta = \frac{1}{4}$ (see the text and eq. (14)). Apart from an upward shift by $\frac{1}{4}$, η^{eff} in (b) is the slope of the curve in (a).

strate this more quantitatively, we plot in fig. 3b the effective exponent

$$\eta_i^{\text{eff}} \equiv 2 - \frac{\log(\chi_{i+1}/\chi_{i-1})}{\log(\xi_{i+1}/\xi_{i-1})}, \quad (14)$$

with $\xi_i \equiv \xi(\beta_i)$ etc. Apart from an upward shift by $\frac{1}{4}$, this is just the slope of the curve in fig. 3a. From the point closest to criticality (corresponding to $\xi \approx 110-140$) we read off the estimate $\eta \approx \eta^{\text{eff}} \approx 0.267$, which is already reasonably close to the KT prediction.

In conclusion, among the two alternatives a pure exponential or a pure power-law critical behavior, we find clear evidence for the former. Estimates of the KT parameters, however, are affected by rather large systematic errors. A significant reduction of these errors would require an enormous computing power.

The numerical simulations were performed on a CRAY X-MP2/4 at the Konrad-Zuse-Zentrum für Informationstechnik Berlin (ZIB) and a CRAY X-MP2/16 at the Computer Center of Universität Kiel.

References

- [1] N.D. Mermin and H. Wagner, Phys. Rev. Lett. 17 (1966) 1133;
- [2] J.M. Kosterlitz and D.J. Thouless, J. Phys. C 6 (1973) 1181; J.M. Kosterlitz, J. Phys. C 7 (1974) 1046; V.L. Berezinskii, Zh. Eksp. Teor. Fiz. 61 (1971) 1144 [Sov. Phys. JETP 34 (1972) 610].
- [3] P. Minnhagen, Rev. Mod. Phys. 59 (1987) 1001; H. Kleinert, Gauge fields in condensed matter, Vol. 1 (World Scientific, Singapore, 1989).
- [4] J. Zittartz, Z. Phys. B 23 (1976) 55, 63; A. Luther and D.J. Scalapino, Phys. Rev. B 16 (1977) 1356; F. Fucito and S. Solomon, Phys. Lett. B 134 (1984) 235.
- [5] A. Patrascioiu and E. Seiler, Phys. Rev. Lett. 60 (1988) 875; E. Seiler, I.O. Stamatescu, A. Patrascioiu and V. Linke, Nucl. Phys. B 305 [FS23] (1988) 623.
- [6] P. Butera, M. Comi and G. Marchesini, Phys. Rev. B 33 (1986) 4725; 40 (1989) 534.
- [7] R. Gupta, J. DeLapp, G.G. Battrouni, G.C. Fox, C.F. Bailie and J. Apostolakis, Phys. Rev. Lett. 61 (1988) 1996.
- [8] U. Wolff, Nucl. Phys. B 322 (1989) 759.
- [9] R.G. Edwards, J. Goodman and A.D. Sokal, Tallahassee preprint FSU-SCRI-90-99, June 1990.
- [10] J. Tobochnik and G.V. Chester, Phys. Rev. B 20 (1979) 3761; J.E. Van Himbergen and S. Chakravarty, Phys. Rev. B 23 (1981) 359; S. Samuel and F.-G. Yee, Nucl. Phys. B 257 [FS14] (1985) 85; P. Harten and S. Suranyi, Nucl. Phys. B 265 [FS15] (1986) 615; J.F. Fernández, M.F. Ferreira and J. Stankiewicz, Phys. Rev. B 34 (1986) 292.
- [11] S. Ami and H. Kleinert, Phys. Rev. B 33 (1986) 4692.
- [12] J.V. José, L.P. Kadanoff, S. Kirkpatrick and D.R. Nelson, Phys. Rev. B 16 (1977) 1217; T. Ohta and K. Kawasaki, Prog. Theor. Phys. 60 (1978) 365; I. Nakayama and T. Tsuneto, Prog. Theor. Phys. 63 (1980) 402; J.L. Cardy and N. Parga, J. Phys. C 13 (1980) 571.
- [13] D.J. Amit, Y.Y. Goldschmidt and G. Grinstein, J. Phys. A 13 (1980) 585; L.P. Kadanoff and A.B. Zisook, Nucl. Phys. B 180 [FS2] (1981) 61.
- [14] J. Villain, J. Phys. (Paris) 36 (1975) 581.
- [15] W. Janke and H. Kleinert, Phys. Rev. B 41 (1990) 6848.
- [16] W.J. Shugard, J.D. Weeks and G.H. Gilmer, Phys. Rev. Lett. 41 (1978) 1399, 1577(E)
- [17] R.H. Swendsen and J.S. Wang, Phys. Rev. Lett. 58 (1987) 86.
- [18] U. Wolff, Phys. Rev. Lett. 62 (1989) 361.
- [19] U. Wolff, Nucl. Phys. B 334 (1990) 581.
- [20] W.H. Press, B.P. Flannery, S.A. Teukolsky and W.T. Vetterling, Numerical recipes - the art of scientific computing (Cambridge Univ. Press, Cambridge, 1986).